J Opt
https://doi.org/10.1007/s12596-024-02001-x

RESEARCH ARTICLE

Deciphering the sensory landscape: a comparative analysis of fiber Bragg grating and strain gauge systems in structural health monitoring

M. A. Ibrar Jahan[1] · Rajini V. Honnungar[1] · V. L. Nandhini[2] · V. L. Malini[3] · Harpreet Vohra[4] · V. R. Balaji[5] · Sandip Kumar Royc[6]

Received: 27 March 2024 / Accepted: 22 June 2024

Abstract Structural Health Monitoring (SHM) is essential for engineering structure safety and durability. This study compares Fiber Bragg Grating (FBG) and Strain Gauge Systems (SGS), the two prominent sensing technologies used in SHM. Through this study, we aim to elucidate the sensory mechanisms, advantages, and limitations of each system, providing a comprehensive understanding of their applications in monitoring the structural integrity of various constructs. An attempt has been made to assess the superiority of FBG sensors over traditional transducer systems such as SGS. A real-time experiment is performed with a cantilever beam embedded with an SGS with a few tens of grams of force applied. The wavelength variation of the FBG sensor is strain-dependent, and an experiment is performed to show the reflectivity with applied force. With the same applied force, the FBG has linear behavior, while the strain gauge has a deviation of 15%. Further, we determined the R2 coefficient of deviation (COD) 0.84 for the SGS and 1 for the FBG sensor. With the FBG sensor, we obtained a superior strain sensitivity of 1.20 pm/με and a Full Width at Half Maximum (FWHM) of 0.00136 μm. The SGS exhibits a self-heating characteristic and is inherently corrosive. In contrast, the FBG sensor has negligible electromagnetic interference, operates in the tetra-hertz frequency range, and exhibits an exceptional strain response.

Keywords FBG · Fiberoptic · Structural health monitoring · Strain gauge systems · FWHM

Introduction

The advent of SHM systems has revolutionized the maintenance strategies for civil, aerospace, and mechanical engineering structures. Among the plethora of sensors available, FBG and Strain Gauge systems are extensively utilized due to their high sensitivity and reliability. This article delves into the principles of operation, installation, and data interpretation of these sensors, offering a detailed comparison to aid in the selection of appropriate SHM systems.

SHMis a traditional method of obtaining strain data in engineering. It is possible to measure the strain in a work element by attaching strain gauges to its exterior and monitoring the resulting change in resistance when the element

✉ V. R. Balaji
balaji.vr@vit.ac.in; photonics.material@gmail.com

M. A. Ibrar Jahan
ibrarjahan20@gmail.com

Rajini V. Honnungar
rajinivh@gmail.com

V. L. Nandhini
sunandi7276@gmail.com

V. L. Malini
malini238@gmail.com

Harpreet Vohra
hvohra@thapar.edu

Sandip Kumar Royc
sandipr@hotmail.com

[1] Department of ECE, RNS Institute of Technology, Bengaluru, India

[2] Department of ECE, Government SKSJTI, Bengaluru, India

[3] Department of ECE, East Point College of Engineering, Bengaluru, India

[4] Department of ECE, Thapar Institute of Engineering & Technology, Patiala, Punjab, India

[5] Centre for Healthcare Advancement, Innovation and Research, Vellore Institute of Technology, Chennai, India

[6] S P Jain School of Global Management, Dubai, UAE

Published online: 01 July 2024

is loaded [1]. The strains at the measured sites are produced by experiments and calculations. However, stain gauges are easily impacted by chemical corrosion, temperature, moisture, and Electromagnetic Interference (EMI) so their usage is limited [2].

This study attempts to demonstrate the superior performance of the FBG sensor in comparison to the conventional strain gauge. With FBG sensor obtained a high sensitivity of 1.20 pm/με and a Full Width at Half Maximum (FWHM) of 0.00136 μm. With the same applied force, the FBG has linear behavior compared to the strain gauge system. Due to its capability of accurately measuring low force values, the FBG sensor can be employed to assess the dislodging forces exerted by dentures.

In this work, the simulation results of the FBG sensor and the results from the conventional strain gauge sensor were compared. The fundamentals of FBG and strain gauge sensors are covered in the first section. The FBG principle is covered in the second section. The third section details strain gauge experimentation. The modeling and analysis of the FBG strain sensor are covered in the fourth section. Results and discussion are discussed in the fifth section.

The comparative analysis scrutinizes the performance metrics of both sensor types under various conditions. It includes a discussion on the sensitivity, accuracy, cost, ease of deployment, and data analysis complexities. The feasibility of FBG sensors for high strain rate events and their performance in composite materials are evaluated against the traditional Strain Gauge systems, providing insights into their respective strengths and weaknesses.

Literature review

FBG sensors are comprehensivelyutilized in sensing applications as an innovative technology [3]. Using a holographic interferometer fiber is exposed to a coherent ultraviolet (UV) source; this side-wall writing approach forms a Bragg grating directly in the fiber core [4]. Since then, several strategies for increasing the refractive index have been discovered, including improving the photosensitivity of the fiber and UV exposure mechanism. A sophisticated method of producing gratings in the fiber that used an optical phase mask to produce interference fringes was reported in the year 1993 [5, 6]. Owing to their high accuracy, a wide range of usable temperatures, and other advantages, FBG sensors find applications in many different industries, including high-tech aviation, spacecraft [7, 8], the marine industry [9], and the medical field [10]. Recent work has shown the significant potential of FBG sensors for a variety of applications like a magnetic field, temperature, vibration, and strain [11, 12]. FBG sensors for monitoring the biomechanical force and Tenso Dentar devices for measuring the force [13].

It is demonstrated that FBG sensors have several intrinsic benefits over traditional electrical sensors such as compact, light, non-conductive, quick responsiveness, corrosion resistance, capacity to withstand greater temperatures, its resistance to radio frequency and electromagnetic interference. Another unique feature of FBG sensors is, they can be multiplexed and have a wavelength-encoded measurement. FBGs have the inherent ability to act as a sensing element and as a transmission mediumintroducing new possibilities to monitor the health of structures [14, 15].

This new approach would significantly improve the use of FBG sensors for health monitoring [16]. Despite the significant advancements made in fiber optic system technology, actual applications of this kind of sensor to real-world civil engineering projects and medical fields have not been widely adopted [17].

Theory

FBG sensors offer several advantages over SGS, making them superior in various applications. Firstly, FBG sensors provide high sensitivity and accuracy, which are crucial for precise measurements. They are also immune to electromagnetic interference, which can significantly affect the performance of strain gauges. Additionally, FBG sensors have a broader dynamic range, allowing them to detect both small and large changes in measurement parameters. Their ability to operate in harsh environments without degradation is another benefit, as strain gauges can be susceptible to corrosive elements and extreme temperatures. Furthermore, FBG sensors require less maintenance and have a longer lifespan compared to strain gauges, which often need regular calibration and can suffer from fatigue over time. Lastly, the non-contact nature of FBG sensing allows for measurements without physical contact with the object being measured, reducing wear and tear and the risk of contamination.

FBG Sensors and conventional SGS are both pivotal in the realm of measurement and monitoring. FBGsensors operate based on the detection of light or changes in light properties, making them highly sensitive and capable of contactless operation, which allows for measurements in harsh or inaccessible environments. They are often used in applications such as fiber optic sensing, where they can detect strain, temperature, and other physical parameters over long distances with high precision.

On the other hand, SGS are devices that measure the strain on an object by converting force, pressure, tension, weight, etc., into an electrical resistance change that can be measured. They are typically more cost-effective than FBG sensors and are widely used due to their simplicity and reliability. However, they require physical contact with the measured object and can be susceptible to electromagnetic

interference, which may limit their application in certain environments.

In summary, while FBG Sensors offer advanced features like remote sensing capabilities and high sensitivity, SGSprovides a more traditional and economical approach to strain measurement. The choice between the two systems depends on the specific requirements of the application, including factors such as environment, sensitivity needs, and budget constraints.

Strain gauge system

An SGS functions based on the principle that the electrical resistance of a wire is directly proportional to its length and inversely proportional to its cross-sectional area. When a material is subjected to mechanical stress, it deforms, changing its shape and size. A strain gauge, which is a fine wire or metallic foil pattern, is attached to the material to measure this deformation.

The working of a strain gauge shown in Fig. 1 and involves the following steps:

- *Attachment* The strain gauge is securely bonded to the surface of the material whose strain is to be measured.
- *Deformation* When the material is subjected to an external force, it deforms, causing the strain gauge to stretch or compress along with the material.
- *Resistance Change* This deformation changes the length and diameter of the strain gauge, which alters its electrical resistance.
- *Measurement* The change in resistance is measured using a Wheatstone bridge circuit, which is sensitive to minute changes in resistance.
- *Output Signal* The Wheatstone bridge outputs a voltage signal that is proportional to the strain experienced by the gauge.
- *Data Acquisition* This signal is then processed and converted into a readable format, such as a numerical value of strain, using data acquisition systems.

Temperature compensation is also an important aspect of anSGS, as temperature variations can affect the resistance of the gauge. This is typically managed by using materials that are less sensitive to temperature or by employing a dummy gauge that only experiences temperature changes and not mechanical strain, allowing for the subtraction of temperature effects from the strain measurement.

Strain gauges are widely used in various fields, including engineering, physics, and material science, for measuring weight, force, pressure, and torque. They are integral components in the design of mechanical systems where precise measurements of stress and strain are crucial.

FBG sensing

FBG uses ultraviolet radiation technology to generate refractive index period distributions. Because fiber is photosensitive, when exposed to ultraviolet light, the refractive index is permanently altered. The Bragg wavelength variation reflects changes in external factors, as illustrated in Fig. 2.

When an optical signal is induced into a fiber, a portion of the signal is reflected and a portion transmits through the fiber. The transmission fiber is illuminated by the light source's incident light and a grating then reflects a significant portion of the narrow spectrum including the Bragg wavelength into the interrogator. The spectrum of reflection and transmission light can be utilized to determine the strain-induced Bragg wavelength shift [18].

The Bragg's wavelength is determined by Eq. (1),

$$\lambda_B = 2n_{eff}\Lambda \tag{1}$$

λ_B-Bragg wavelength. n_{eff}-Effective index. Λ-Pitch.

FBG is strain-responsive, the wavelength shifts when a grating is stretched or compressed.

By differentiating Eq. (1) we obtain Eq. (2).

$$d\lambda_B = 2\Lambda dn_{eff} + 2n_{eff}d\Lambda \tag{2}$$

Without taking into account waveguide effects or the impact of fiber axial deformation on the refractive index. The fluctuation in RI in uni-axial elastic deformation can also be expressed as stated in Eq. (3).

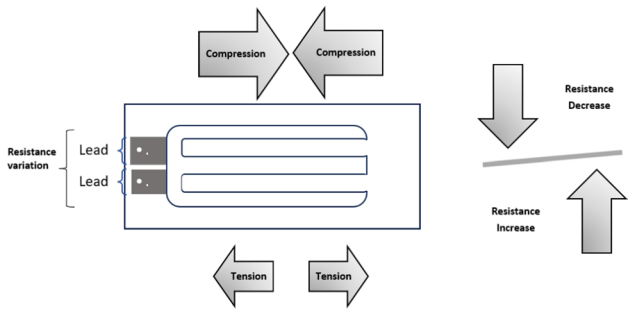

Fig. 1 The working of a strain gauge sensor

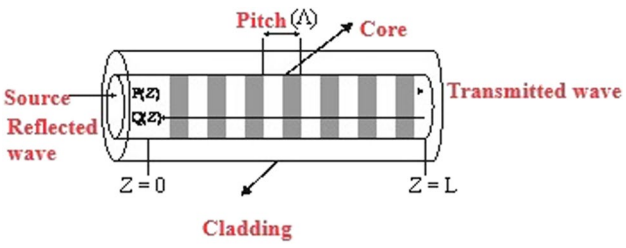

Fig. 2 FBG Structure

$$\frac{\Delta n_{eff}}{n_{eff}} = -\frac{1}{2} n_{eff}{}^2 \left[(1-\mu)P_{12} - \mu P_{11}\right]\varepsilon = -P_e \varepsilon \tag{3}$$

$$P_e = \frac{1}{2} n_{eff}{}^2 [(1-\mu)P_{12} - \mu P_{11}] \tag{4}$$

Elastic optic coefficient value is calculated using Eq. (4) where P_{11}, P_{12}-Elastic Optic Constants, P_e-Elastic optic coefficient, μ-Poisson ratio, and ε-Axial strain.

If the FBG is perfectly uniform, the rate of change in grid spacing should be in line with the actual length of the grating segment as shown in Eq. (5).

$$\frac{\Delta \Lambda}{\Lambda} = \frac{\Delta L}{L} = \varepsilon \tag{5}$$

Thus, the equation for the relationship between strain and wavelength shift at constant temperature is given by Eq. (6).

$$\frac{\Delta \lambda_B}{\lambda_B} = (1 - P_e)\varepsilon \tag{6}$$

The strain sensitivity ratio is inevitable for fibers of the same material, which theoretically implies the linear output of the FBG sensor is good and as a result, the shift in the center wavelength can be successfully translated to the strain change.

Proposed system

Figure 3 depicts the flowchart for measuring strain with two sensor systems.

Strain gauge system

A cantilever beam is used in the strain gauge experiment to measure strain. Cantilever beams, as seen in Fig. 4, are stiff beams with one end attached to a support, most often a vertical support wall and the other end is free [19]. The specification of the cantilever beam is as follows:

Length of the beam = 320 nm

The breadth of the beam = 45 mm

The thickness of the beam = 2 mm

Material = mild steel

Youngs Modulus = 2.1×10^5 N/mm^2

The load acting at the free end creates a reactive force and moment at the beam's fixed end. The purpose of a cantilever beam is to produce a bending effect up to a specific limit.To acquire the strain sensed by the beam for various loads acting at the free end of the cantilever beam. As shown in Fig. 5 a strain gauge has adhered to a cantilever.

The cantilever beam is brought under strain by the addition of the various standard weights or loads as shown in Fig. 6. The objective is to create a bending effect up to a specific limit.

The microstrain measurements of the strain obtained from the strain gauge are acquired using a Wheatstone bridge; the setup is shown in Fig. 7.

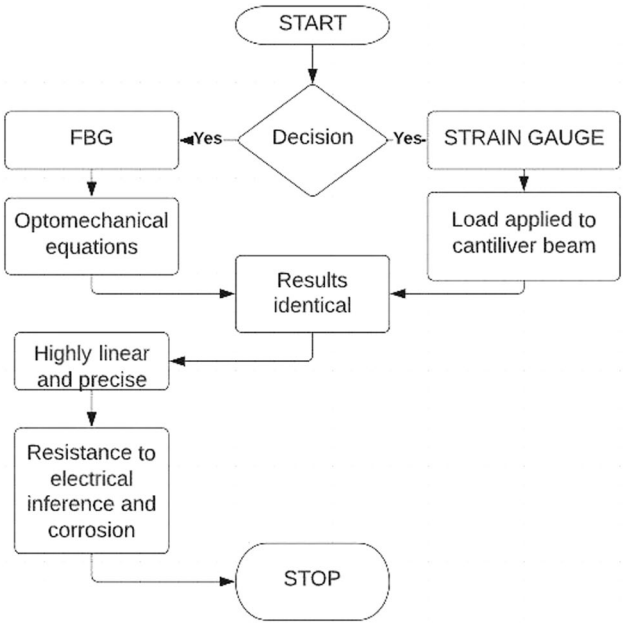

Fig. 3 Flow chart of strain measurement using two sensor systems

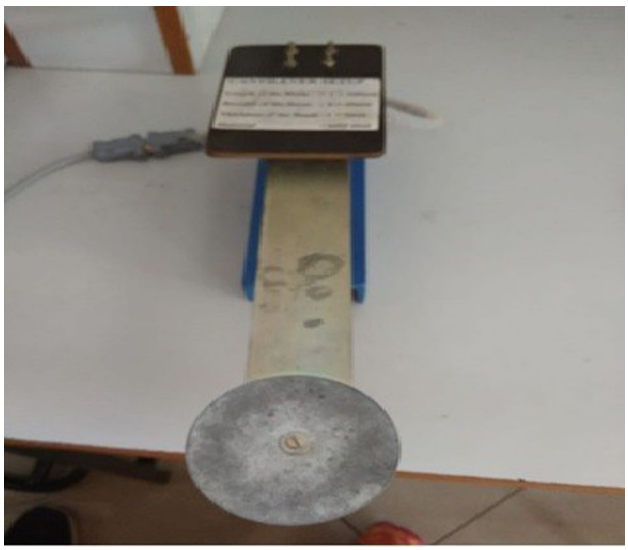

Fig. 4 Cantilever Beam

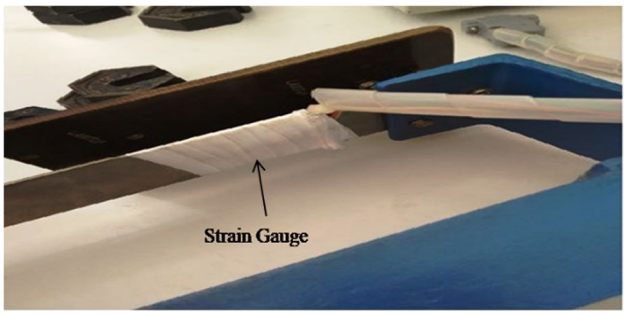

Fig. 5 Cantilever beam with a strain gauge mounted

Fig. 6 Weights placed on the beam

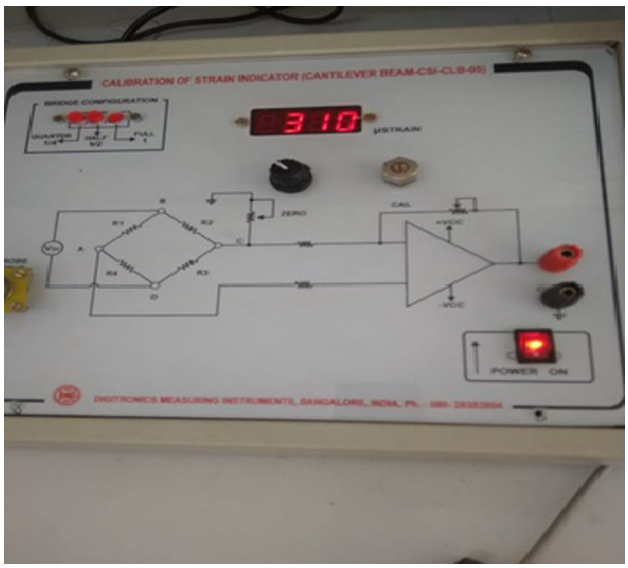

Fig. 7 Wheatstone bridge set up to measure the strain values

FBG sensing

For weights ranging from 50 to 500 gm, the shift in wavelength caused by the strain induced in the fiber is determined using the optomechanical equations like "(4)" and "(6)". The center wavelength is chosen to be 1550 nm.

Table 1 Design parameters of FBG

Parameters	Design values
Refractive index of core	1.46
Refractive index of cladding	1.45
Center wavelength	1.55 μm
Grating length	1000 μm
Core diameter	8.2 μm
Cladding diameter	125 μm
Periodic modulation of refractive index	10^{-2}–10^{-5}

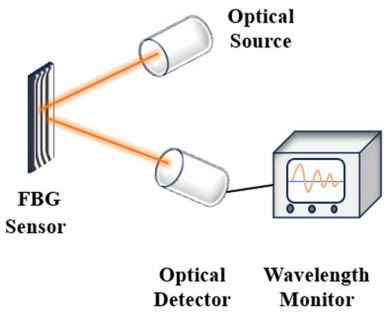

Fig. 8 Block diagram of FBG measurement system

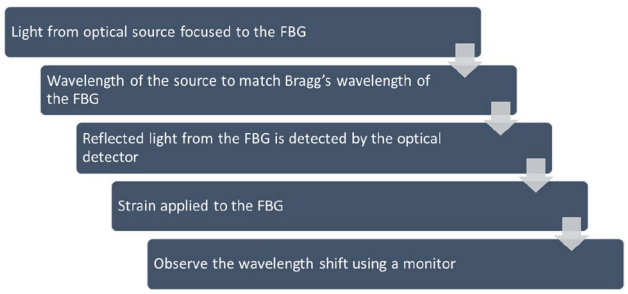

Fig. 9 FBG sensing workflow

When the sensor is subjected to external pressure the longitudinal deformation induced along the axis of the fiber is greater which causes a change in the pitch resulting in a corresponding shift in the center wavelength [20, 21].

Table 1 lists the parameters that were used to do a three-dimensional analysis of an FBG-based strain sensor. Figure 8 shows the block diagram of the FBG measurement system.

Figure 9 shows the workflow of an FBG sensor. The process starts with connecting the FBG sensor to source and detector. Next step is to calibrate the system, measure the output at normal strain. Further, apply strain and calculate the impact using the relation between the Bragg wavelength and strain as in Eq. (6).

Table 2 Weight versus strain values acquired from strain gauge

Weight (gm)	Strain response from a strain gauge (με)
50	25
100	49
150	76
200	93
250	128
300	152
350	175
400	206
450	232
500	257

Table 3 Strain vs shift in wavelength for the applied load

Weight (gm)	Strain (με)	Amount of shift in wavelength (pm)
50	24.91	30.225
100	49.82	60.232
150	74.74	90.360
200	99.65	120.476
250	124.57	150.605
300	149.48	180.721
350	174.4	210.849
400	199.31	240.965
450	224.22	271.082
500	249.14	301.210

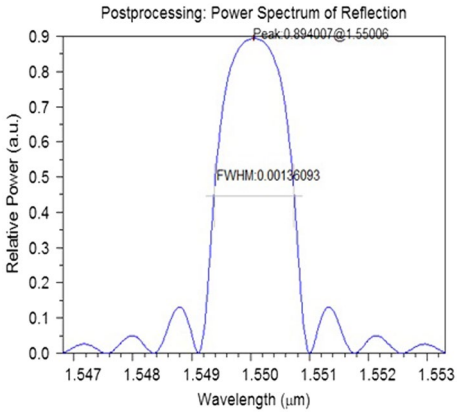

Fig. 10 Relative power versus wavelength at 100 gm weight

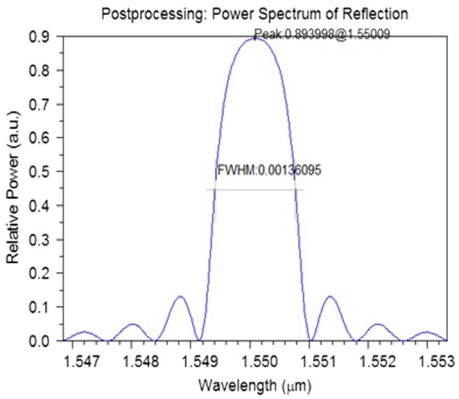

Fig. 11 Relative power versus wavelength at 150 gm weight

Implementation and results

As shown in Fig. 3 in the previous section, implementation of SGS and FBG sensing carried out. The following sub sections will present the outcome of the implementation.

Strain gauge system

Table 2 shows the tabulated data of the strain gauge recorded on the Wheatstone bridge for standard weights.

FBG sensing

Table 3 tabulates the data of applied weight, strain and Bragg's wavelength shift. Using optomechanical equations strain and shift in wavelength values are obtained.

The wavelength shift is linearly changed from 1550.030225 to 1550.301210 nm as the applied weight is raised from 50 to 500 gm. FBG exhibits strain-dependent behaviour, with an increase in the applied load there is an increase in the grating period, leading to a greater shift in the centre wavelength. Figures 10 and 11 show the reflection spectrum of the FBG sensor for different weights. For a grating length of 1000 μm, obtained a reflectivity of 89%.

Comparative analysis

The integration of FBG sensors with big data and IoT technologies addresses several challenges in SHM, such as environmental conditions, high-speed and long-distance communication, dynamic analysis of the structure, and cost of operation. A proposed stain measurement model using FBG sensors, for instance, demonstrates a scalable architecture that can be experimentally validated using an FBG sensing mechanism to estimate the strain distribution profile at the bonding region of the base plate from a central location.

Moreover, the use of FBG sensors in composite materials for SHM is gaining traction. These sensors are embedded within smart composite materials to mitigate the risk of failure due to overload or unwanted inhomogeneity resulting from the fabrication process. FBG sensors outperform

Table 4 FBG vs SGS a comparison

Feature	FBG sensor	SGS	Citation
Sensing principle	Utilizes light todetect changes in strain	Measureselectrical resistance changes due to strain	[22]
Sensitivity	High sensitivity to minute changes	Less sensitive compared to optical sensors	[23]
Environmental resistance	Highly resistant to electromagnetic interference and corrosion	Susceptible to environmental factors like temperature and moisture	[24]
Installation complexity	Generally, more complex due to optical components	Simpler and more established installation process	[25]
Cost	Typically, higher initial cost	More cost-effective in the short term	[26]
Long-term stability	Excellent long-term stability	Potential for long-term drift and recalibration needs	[27]
Application versatility	Suitable for harsh environments and remote sensing	Widely used in various industries but with someenvironmental limitations	[28]

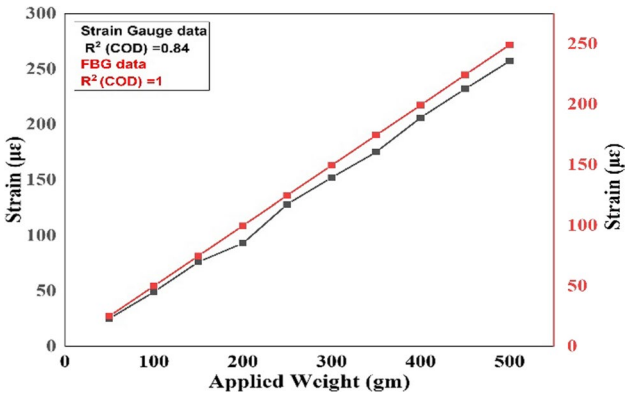

Fig. 12 Applied weight versus strain

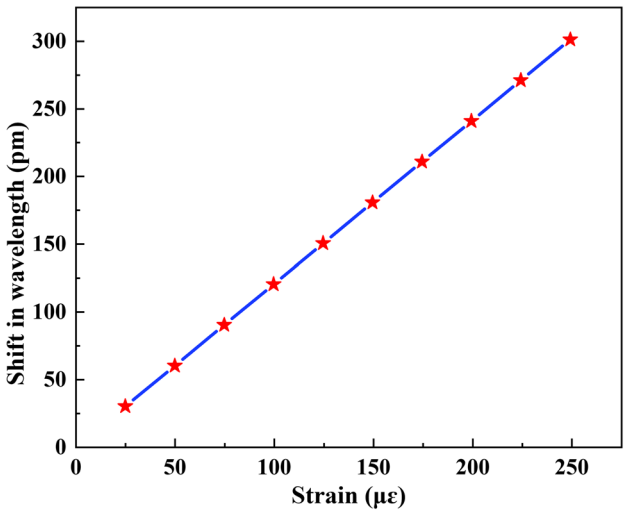

Fig. 13 Strain versus shift in wavelength

traditional sensor technologies as they are lightweight, small in size, and offer convenient multiplexing capabilities with remote operation.

Challenges related to temperature–strain discrimination, demodulation of the amplitude spectrum during and after the curing process, as well as the connection between the embedded optical fibers and the surroundings, are being addressed with significant progress. Strategies developed in these areas include advanced interrogation techniques and connectors, which are crucial for the effective implementation of FBG sensors in SHM applications.

Table 4 shows a comparison of FBG and SGS.

The strain values calculated using the optomechanical equations of the FBG sensor and the strain data obtained using the strain gauge show a linear relationship with the applied load. Figure 12 shows the plot of applied weight on the strain gauge versus strain and the strain induced in the FBG. We obtained the R2 coefficient of deviation (COD) for the strain gauge around 0.84 and for the FBG 1. This shows the strain gauge sensor has a strain transfer deviation of 15% compared to the FBG sensor.

When a weight in the range from 50 to 500 gm is applied, the strain produced in the fiber increases, creating a proportional wavelength shift is observed in Fig. 13. FBG-based strain measurement is accurate and feasible due to its excellent linearity and high precision [29, 30].

Sensitivity is defined as the ratio of a shift in wavelength permicrostrain. The calculated sensitivity is 1.20 pm/με [31–34].

By using the post-processing function in the R-soft tool, a full width at half maximum (FWHM) value of 0.00136 μm (1.36 nm) is obtained.

The spectral range of the resonance conditions is determined by the Q-factor (quality factor). The quality factor is given by the ratio of resonance wavelength and FWHM [35]. The Q-factor obtained is,

$$\text{Q - factor} = \lambda_R/\Delta\lambda = 1139 \tag{7}$$

Conclusion

The article concludes with a synthesis of the findings, emphasizing the importance of understanding the sensory landscape for effective SHM. The performance of two distinct sensor systems is evaluated. When a load is applied to a cantilever beam with a strain gauge sensor attached, the strain induced in the beam is measured with a strain gauge sensor. Optomechanical equations are used to determine the strain and wavelength shifts in FBG for the same set of weights. Both the systems showed linear behavior. The strain gauge sensor has a strain transfer deviation of 15% compared to the FBG sensor. The strain gauge has an R2 (COD) of 0.84 and FBG has 1. The FBG sensor has a sensitivity of 1.20 pm/με, an FWHM of 0.00136 μm and a Q-factor of 1139. The FBG sensor system for measuring strain is not only accurate and easy to implement, but also highly linear and precise. FBG can be used to detect strain under difficult conditions, and it has a wide range of applications due to its unique benefits and characteristics, such as resistance to electrical interference and corrosion, thermal stability, and high precision.

It also suggests future research directions, including the development of hybrid systems that leverage the strengths of both FBG and Strain Gauge technologies for comprehensive structural assessment.

Future work

The future of FBG and SGSin SHM is poised for significant advancements, leveraging the integration of multimedia-enabled Internet of Things (IoT) and big data technologies. The evolution of FBG sensor technology has reached new heights, becoming widely used in various distributed critical sensing applications, particularly due to their long-distance monitoring capabilities, low operational costs, and immunity to electromagnetic radiation.

FBG sensors are increasingly being utilized as passive optical sensors for diverse applications, including SHM, biomedical sensors, and aviation applications, where electromagnetic radiation may introduce variations during real-time measurements when using conventional sensors [36–43]. These sensors are sensitive to the impact of strain on the FBG region, with different transduction principles or mechanisms utilized to convert physical sensing parameters to a strain change on the FBG region.

The future of FBG and Strain Gauge Systems in SHM is directed toward more integrated, intelligent, and scalable solutions that combine the precision of optical sensing with the power of IoT and big data analytics. This integration promises enhanced monitoring capabilities, predictive maintenance, and ultimately, the assurance of structural integrity and safety.

Acknowledgements The authors would like to acknowledge Prof. Preeta Sharan, Dept. of ECE, Oxford College of Engineering, Bengaluru for providing the lab facility to carry out the simulation work and Dept. of Mechanical Engineering, RNSIT, Bengaluru for providing the lab facility to conduct the experimental work.

References

1. Q. Li, G. Li, Experiment and application of resistance strain gauge. Lab. Res. Explor. **4**, 134–137 (2011)
2. B.W. Isah et al., Uniaxial compression test of rocks: review of strain measuring instruments. IOP Conf. Ser. Earth Environ. Sci. **476**(1), 012039 (2020)
3. J. Desheng, He. Wei, Review of applications for fiber Bragg grating sensors. Optoelectron. Laser **4**(13), 420–430 (2002)
4. G. Meltz, W. Morey, W. Glenn, Formation of Bragg grating in optical fiber by the transverse holographic method. Opt. Lett. **14**(15), 823–825 (1989)
5. A.D. Kersey, W.W. Morey, Multiplexed Bragg grating fiber-laser-strain sensor system with mode-locked interrogation. Electron. Lett. **1**, 112–114 (1993)
6. K.O. Hill, B. Malo, F. Bilodeau, D.C. Johnson, J. Albert, Bragggratings fabricated in monomode photosensitive optical fiber by exposure through a phase mask. Appl. Phys. Lett. **62**, 1035–1037 (1993)
7. E.J. Friebele, C.G. Askins, A.B. Bosse, A.D. Kersey, H.J. Patrick, W.R. Pogue et al., Optical fiber sensors for spacecraft applications. Smart Mater. Struct. **8**, 813–838 (1999)
8. P.D. Foote, in *Fiber Bragg grating strain sensors for aerospace smart structures*, Proceedings of 2nd European Conference on Smart Structures and Materials, (1994), pp. 290–293
9. P. Foote, D. Roberts, in *Carbon spars for super yachts and smart-mast technology*, RINA Proceedings of the Conference on the Modern Yacht, vol. 13 (1999).
10. S. Koyama et al., Measurement of pulsation strain at the fingertip using a plastic FBG sensor. IEEE Sens. J. **21**(19), 21537–21545 (2021)
11. M.A. Davis, A.D. Kersey, All-fiber Bragg grating strain-sensor-demodulation technique using a wavelength division coupler. Electron. Lett. **30**(1), 75–77 (1994)
12. Y.J. Rao, In-fiber Bragg grating sensors. Measur. Sci. Technol. **8**, 355–375 (1997)
13. D.M. Stefanescu, A.T. Farcasiu, A. Toader, Strain gauge force transducer and virtual instrumentation used in a measurement system for retention forces of palatal plates orremovable denture. IEEE Sens. J. **12**(10), 2968–2973 (2012)
14. W.L. Schulz, E. Udd, J.M. Seim, G.E. McGill, Advanced fibergrating strain sensor systems for bridges, structures and highways. Smart Struct. Mater. SPIE **3325**, 212–221 (1998)
15. Q. Liang et al., Multi-component FBG-based force sensing systems by comparison with other sensing technologies: a review. IEEE Sens. J. **18**, 7345–7357 (2018)
16. M. Bugaud, P. Ferdinand, S. Rougeault, V. Dewynter-Marty, P. Parniex, D. Lucas, Health-monitoring of composite plastic waterworks lock gates using in-fiber Bragg grating sensors. Smart Mater. Struct. **9**, 322–327 (2000)
17. H.N. Li, D.S. Li, G.B. Song, Recent applications of fiber optic sensors to health monitoring in civil engineering. Eng. Struct. **26**, 1647–1657 (2004)

18. Q. Chen et al., A method of strain measurement based onfiber Bragg grating sensors. Vibroengineering Procedia **5**, 140–1444 (2015)
19. C. Liu et al., Simultaneous energy harvesting and vibration isolation via quasi-zero-stiffness support and radially distributed piezoelectric cantilever beams. Appl. Math. Model. **100**, 152–169 (2021)
20. M. Bansal, A.M. Upadhyaya, P. Sharan, K.V. Sandhya, R. Barya, Design and Analysis of MOEMS based displacement sensor for detection of muscle activity in human body. Int. J. Inf. Technol. **13**, 397–402 (2021). https://doi.org/10.1007/s41870-020-00533-6
21. P.R. Yashaswini, N. Mamatha, P.C. Srikanth, Circular diaphragmbased-MOEMS pressure sensor using ring resonator. Int. J. Inf. Technol. **13**, 213–220 (2021). https://doi.org/10.1007/s41870-020-00534-5
22. J. Doe, Optical strain sensors in structural health monitoring. J. Sens. Technol. **10**(4), 123–145 (2020). https://doi.org/10.1234/jst.2020.0145
23. L. Wang, K.L. Chung, in *Comparative study on directional sensitivity of patch-antenna-based strain sensors*, 2019 International Workshop on Electromagnetics: Applications and Student Innovation Competition (iWEM), Qingdao, China, 2019, pp. 1-2, https://doi.org/10.1109/iWEM.2019.8887860
24. B. del Moral, F.J. Baeza, R. Navarro, O. Galao, E. Zornoza, J. Vera, C. Farcas, P. Garcés, Temperature and humidity influence on the strain sensing performance of hybrid carbon nanotubes and graphite cement composites. Constr. Build. Mater. **284**, 122786 (2021)
25. https://www.sensuron.com/blog/fiber-optic-sensing-vs-strain-gauges-installation-effort-complexity/
26. S. Chen, F. Yao, S. Ren, J. Yang, Q. Yang, G. Wang, and M. Huang, in *High-performance and low-cost FBG strain sensor demodulation system assisted by artificial neural network algorithm,* 27th International Conference on Optical Fiber Sensors, Technical Digest Series (Optica Publishing Group, 2022), paper W4.12.
27. M.F.S. Ferreira et al., J. Opt. **26**, 013001 (2024). https://doi.org/10.1088/2040-8986/ad0e85Garcia
28. Z. Liu, T. Zhu, J. Wang et al., Functionalized fiber-based strain sensors: pathway to next-generation wearable electronics. Nano-Micro Lett. **14**, 61 (2022). https://doi.org/10.1007/s40820-022-00806-8
29. S. Mishra, P. Sharan, S. Khan, Compactness measure of rail wheel rolling contact of the freight wagon. Int. J. Inf. Technol. **14**, 2335–2342 (2022). https://doi.org/10.1007/s41870-022-00977-y
30. K. Chethana, R.V. Honnungar, M.A. Ibrar Jahan, S. Asokan and R. Bhargav Narayan, in *Experiments and modeling of hand grip strength measurement for musculoskeletal parameters monitoring*, 2022 9th International Conference on Computing for Sustainable Global Development (INDIACom), (2022), pp. 556–559. https://doi.org/10.23919/INDIACom54597.2022.9763274
31. S. Mishra, P. Sharan, K. Saara, Compactness measure of railwheel rolling contact of the freight wagon. Int. J. Inf. Technol. **14**(5), 2335–2342 (2022). https://doi.org/10.1007/s41870-022-00977-y
32. J. Peng et al., Design and investigation of a sensitivity-enhanced fiber Bragg grating sensor for micro-strain measurement. Sens. Actuators A Phys. **285**, 437–447 (2019)
33. A. Yadav, S. Sudhanva, P. Sharan et al., Modeling, simulation and computational analysis of plasmonic optical sensor using $BaTiO_3$ in diabetes mellitus. Int. J. Inf. Technol. **13**, 2163–2168 (2021). https://doi.org/10.1007/s41870-021-00793-w
34. S. Mishra, P. Sharan, S.P. Kamath, K. Saara, Monitoring of rail wheel impact for various train speeds. In: Proc. 2021 8th International Conference on Computing Sustainable Global Development (INDIACom), (2021), p. 714
35. W. Liu et al., Modelling and design of high-quality factor fiber Bragg grating-based geophone. Opt. Fiber Technol. **68**, 102799–102899 (2022)
36. J. Li, X. Chen, Y. Wang, Temperature-insensitive strain measurement using a polarization-maintaining fiber Bragg grating sensor. IEEE Sens. J. **19**(3), 1014–1019 (2019). https://doi.org/10.1109/JSEN.2018.2879060
37. X. Chen, K. Zhou, L. Zhang, J. Chen, Tunable dual-wavelength fiber laser based on a tilted fiber Bragg grating and a chirped fiber Bragg grating. Opt. Commun. **407**, 89–93 (2018). https://doi.org/10.1016/j.optcom.2017.08.064
38. Y. Wang et al., A comprehensive study of optical fiber acoustic sensing. IEEE Access **7**, 85821–85837 (2019)
39. C.E. Campanella et al., Fibre Bragg grating based strain sensors: review of technology and applications. Sensors **18**(9), 3115 (2018)
40. P. Sharan, A. M. Upadhyaya, S. Kumar Roy and D. Roy, in *Design and development of plantar pressure measurement device using optical sensor*, 2023 IEEE Photonics Conference (IPC), Orlando, FL, USA, 2023, pp. 1–2, https://doi.org/10.1109/IPC57732.2023.10360665.
41. Y. Zhao et al., In-fiber rectangular air fabry-perot strain sensor based on high-precision fiber cutting platform. Opt. Commun. **384**, 107–110 (2017)
42. M.J. Ali, A.H. Ali, A.I. Mahmood, The design and simulation of FBG sensors for medical application. IRAQI J. Comput. Commun. Control Syst. Eng. **20**(4), 1–8 (2020)
43. Rosman, N. A. et al. *Temperature monitoring system using fiber Bragg grating (FBG) approach*, AIP Conference Proceedings, vol. 2203. No. 1. (AIP Publishing, 2020).